Statistical modeling and MAP estimation for body fat quantification with MRI ratio imaging

Wilbur C. K. Wong[a], David H. Johnson[a], David L. Wilson*[a,b]
[a]Department of Biomedical Engineering, Case Western Reserve University, Cleveland, OH USA 44106;
[b]Department of Radiology, University Hospitals of Cleveland and Case Western Reserve University, Cleveland, OH USA 44106

ABSTRACT

We are developing small animal imaging techniques to characterize the kinetics of lipid accumulation/reduction of fat depots in response to genetic/dietary factors associated with obesity and metabolic syndromes. Recently, we developed an MR ratio imaging technique that approximately yields $\mathrm{lipid}/\{\mathrm{lipid}+\mathrm{water}\}$. In this work, we develop a statistical model for the ratio distribution that explicitly includes a partial volume (PV) fraction of fat and a mixture of a Rician and multiple Gaussians. Monte Carlo hypothesis testing showed that our model was valid over a wide range of coefficient of variation of the denominator distribution ($c.v.: 0-0.20$) and correlation coefficient among the numerator and denominator (ρ: $0-0.95$), which cover the typical values that we found in MRI data sets ($c.v.$: $0.027-0.063$, ρ: $0.50-0.75$). Then a maximum *a posteriori* (MAP) estimate for the fat percentage per voxel is proposed. Using a digital phantom with many PV voxels, we found that ratio values were not linearly related to PV fat content and that our method accurately described the histogram. In addition, the new method estimated the ground truth within $+1.6\%$ vs. $+43\%$ for an approach using an uncorrected ratio image, when we simply threshold the ratio image. On the six genetically obese rat data sets, the MAP estimate gave total fat volumes of $279 \pm 45\mathrm{mL}$, values $\approx 21\%$ smaller than those from the uncorrected ratio images, principally due to the non-linear PV effect. We conclude that our algorithm can increase the accuracy of fat volume quantification even in regions having many PV voxels, e.g. ectopic fat depots.

Keywords: Classification, segmentation, statistical methods, Monte Carlo hypothesis testing, fat quantification, maximum *a posteriori* estimate

1. PURPOSE

We are developing small animal imaging techniques to characterize the kinetics of lipid accumulation/reduction of fat depots (visceral, subcutaneous, muscular, etc.) in response to genetic/dietary factors associated with obesity and metabolic syndromes. Quantitative analysis of body fat is therefore vital to the study. Such imaging and analysis protocols are also beneficial to various epidemiological studies [1, 2, 3]. Volumetric information and distribution of the fat are important determining factors of the health risks related to obesity, such as diabetes, cardiovascular and cerebrovascular diseases. Recently, we developed a ratio imaging technique, which based upon spin echo sequence and two MRI acquisitions, to provide an estimate of lipid content per voxel [4]. Our method is inherently free from phase artifact (we use only magnitude images) and signal intensity bias field, and is less sensitive to chemical shift artifact than the Dixon method. Also, it produces relatively high signal-to-noise ratio (SNR) images as compared to chemically selective excitation pulses. One of our studies shows that the method provides reproducible volumetric measurement of fat depots. A ratio image is computed by dividing a "fat only" T1-weighted image by a "fat+water" counterpart on a pixel-by-pixel basis. The chemical shift selective (CHESS) pulses [5] are used to produce the "fat only" image with negligible water signal.

In the present work, we investigate the statistical distribution of the ratio intensity and develop a model for it. The goodness-of-fit is assessed with Monte Carlo hypothesis testing. We also invalidate the linearity assumption on the ratio intensity and the lipid content with numerical phantom and MRI data sets from animal experiments. A maximum *a*

*david.wilson@case.edu; phone 1 216 368-4009; fax 1 216 368-4969; bme.case.edu/bmil/

posteriori (MAP) estimate for the percentage of fat per voxel from the ratio images is proposed. Experimental results show that our estimate is capable of correcting the non-linearity and producing fat content estimates at each voxel. Furthermore, it increases the accuracy of fat volume quantification.

2. METHODS

MRI magnitude in the presence of noise was shown to be a Rician distributed random variable due to the nonlinear mapping of the real and imaginary signals [6]. This finding opens opportunity for statistical modeling of MRI magnitudes to applications such as image segmentation [7]. Gudbjartsson and Patz [6] suggested that if the signal-to-noise ratio (SNR) is larger than two, the magnitude is approximately Gaussian distributed; SNR is defined as A/σ_n, where A is the truth magnitude (magnitude image intensity in the absence of noise) and σ_n denotes the standard deviation of the Gaussian noise in the real and imaginary images.

In this section, we begin by presenting the statistical models of (1) pure tissue class and (2) mixture of two pure tissue classes in ratio MRI magnitude image. Finally, we construct a finite mixture model of the magnitude ratio image in the context of fat quantification with MRI and propose a method to calculate the percentage of fat in each voxel.

2.1 Ratio of Two Gaussian Distributed Magnitudes

We start the statistical modeling of the ratio of two MRI magnitudes with the Gaussian distribution. Suppose Y and X are two Gaussian distributed random variables with means μ_i, variances σ_i, $(i \in \{x, y\})$ and correlation coefficient ρ, and $W_R = Y/X$ is the ratio of the two random variables. The theoretical distribution with zero means was given in the seminal work by Geary [8]. Fieller [9] and Marsaglia [10] later investigated a general exact formulation of the distribution with non-zero means. The standard approximation of the distribution were considered by Hinkley [11]. Hayya *et al.* [12] further suggested that if the coefficient of variation of X, $c.v.(X)$, is small, such distribution approximates normality. The rationale is straightforward, as under such condition, the denominator approaches a constant, thus the quotient approaches a Gaussian distribution (in general, the same kind of distribution as the numerator). The statistical modeling of the ratio MRI signals in this paper is built upon such normal approximation. According to the approximation [12], $W_R \sim \mathcal{N}\left(\mu_r, \sigma_r^2\right)$, where

$$\begin{aligned} \mu_r &= \frac{\mu_y}{\mu_x} + \frac{\sigma_x^2 \mu_y}{\mu_x^3} - \frac{\rho \sigma_x \sigma_y}{\mu_x^2} \\ \sigma_r^2 &= \frac{\sigma_x^2 \mu_y^2}{\mu_x^4} + \frac{\sigma_y^2}{\mu_x^2} - \frac{2\rho \sigma_x \sigma_y \mu_y}{\mu_x^3}. \end{aligned} \tag{1}$$

In this work, we assume the correlation coefficient $\rho = 0$ to simplify the parameter estimation. Later in Section 3, we validate such assumption with Monte Carlo hypothesis testing.

2.2 Ratio of Two Mixture Magnitudes

Since the mixture of two Gaussian distributed random variables is also Gaussian distributed, by following the formulation presented in Section 2.1, we derive the normally approximated distribution $W_{R'}$ to model the ratio distribution of the magnitude of two mixtures. Let $X_i \sim \mathcal{N}\left(\mu_{x:i}, \sigma_{x:i}^2\right)$ and $Y_i \sim \mathcal{N}\left(\mu_{y:i}, \sigma_{y:i}^2\right)$ $(i \in \{1, 2\})$ be four Gaussian distributed random variables, where i is the class index. X_1 and X_2 compose a mixture with composition variable $\alpha \in [0, 1]$ (denotes the proportion of X_2 in the mixture), and same for Y_1 and Y_2. The means and variances of the mixtures are then expressed as,

$$\begin{aligned}
\mu_{x;\alpha} &= (1-\alpha)\,\mu_{x:1} + \alpha\mu_{x:2} \\
\sigma^2_{x;\alpha} &= (1-\alpha)^2\,\sigma^2_{x:1} + \alpha^2\sigma^2_{x:2} \\
\mu_{y;\alpha} &= (1-\alpha)\,\mu_{y:1} + \alpha\mu_{y:2} \\
\sigma^2_{y;\alpha} &= (1-\alpha)^2\,\sigma^2_{y:1} + \alpha^2\sigma^2_{y:2}.
\end{aligned} \tag{2}$$

By substituting all these means and variances into Equations (1) (assume $\rho = 0$), we have the mean and variance of the normally approximated distribution $W_{R'}$ as follow,

$$\begin{aligned}
\mu_\alpha &= \frac{\mu_{y;\alpha}}{\mu_{x;\alpha}} + \frac{\sigma^2_{x;\alpha}\mu_{y;\alpha}}{\mu^3_{x;\alpha}} \\
\sigma^2_\alpha &= \frac{\sigma^2_{x;\alpha}\mu^2_{y;\alpha}}{\mu^4_{x;\alpha}} + \frac{\sigma^2_{y;\alpha}}{\mu^2_{x;\alpha}}.
\end{aligned} \tag{3}$$

Finally, we marginalize the variable α to obtain the probability density function (pdf) of the ratio of two mixture signals,

$$f(z) = \frac{1}{Z}\int_0^1 h(\alpha)\, g\left(z;\mu_\alpha,\sigma^2_\alpha\right) d\alpha, \tag{4}$$

where z is the signal ratio variable, Z is a normalization constant and $h : [0,1] \rightarrow [0,1]$ is a weighting function of the normally approximated distribution $W_{R'}$ at various compositions. This marginalization between 0 and 1 is based on a general assumption that the values of the composition variable α may have different chance of occurrence in its domain. Such chance is denoted by $h(\alpha)$ and therefore we have a constraint on h,

$$\int_0^1 h(\alpha)\, d\alpha = 1. \tag{5}$$

This is similar to the method of Santago and Gage [13] in which they focused on the magnitude pdf of partial volume voxels. By assuming the boundary between the tissues is arbitrarily located within the mixture voxel, they marginalize the magnitude pdfs of various mixture compositions with a constant weighting function.

2.3 The Finite Mixture Model (FMM)

We follow the derivation given in Section 2.1 to model the distribution of the magnitude ratio ($M_{\mathrm{f}}/M_{\mathrm{fw}}$) in pure fat regions (cf. Equation (1), y denotes "fat only", x denotes "fat+water" and r denotes the magnitude ratio). This is justified by the fact that the SNR of those regions is high enough to give a good distribution approximation with the Gaussian pdf. However, for the pure water regions, SNR in $\mathcal{I}_{\mathrm{f}}$ is small, Gaussian distribution does not give good approximation. One has to model the magnitude variation of M_{f} with Rician distribution [6]. In this work, it is reasonable to further assume that the distribution of $M_{\mathrm{f}}/M_{\mathrm{fw}}$ in the pure water regions is Rician. This is because the coefficient of variation of the denominator (M_{fw}) is small (cf. Section 2.1). Statistical modeling of the mixture classes in ratio images is problematic. When α is small, i.e. large portion is water, SNR of M_{f} may not large enough for a good Gaussian approximation. Nevertheless, as this only contributes a small portion in the whole image volume, we approximate its distribution with a Gaussian pdf to not over-complicate the modeling. As such, we use the pdf in Equation (4) to model the ratio distribution of the mixture classes (cf. Equations (2) and (3), y denotes "fat only", x denotes "fat+water", class 1 denotes pure water and class 2 denotes pure fat).

The overall formulation of the finite mixture model (FMM) that describes the magnitude ratio distribution becomes the following,

$$p(z) = a_{\mathrm{f}} g\left(z; \mu_{\mathrm{f}}, \sigma_{\mathrm{f}}^2\right) + a_{\mathrm{m}} f(z) + a_{\mathrm{w}} r\left(z; v_{\mathrm{w}}, \sigma_{\mathrm{w}}^2\right) \tag{6}$$

where

$$\sum_{i \in \{\mathrm{f},\mathrm{m},\mathrm{w}\}} a_i = 1, \quad 0 \le a_i \le 1, \forall i. \tag{7}$$

$$r\left(z; v_{\mathrm{w}}, \sigma_{\mathrm{w}}^2\right) = \frac{z}{\sigma_{\mathrm{w}}^2} \exp\left(\frac{-\left(z^2 + v_{\mathrm{w}}^2\right)}{2\sigma_{\mathrm{w}}^2}\right) I_0\left(\frac{z v_{\mathrm{w}}}{\sigma_{\mathrm{w}}^2}\right) \tag{8}$$

where a_i ($i \in \{\mathrm{f}, \mathrm{m}, \mathrm{w}\}$) are the weights of the three sub-models, the subscript f, m and w denote the parameters for pure fat, mixture of fat and water, and pure water, respectively. The parameters μ_{f} and σ_{f}^2 are the mean and variance of the Gaussian distribution $g(\cdot)$ (cf. Equation (1), assuming $\rho = 0$) that models the ratio variation in the pure fat class. $f(\cdot)$ is the statistical model of the mixture classes (cf. Equation (4)). The function $r(\cdot)$ is the Rician distribution, v_{w} is the magnitude of the underlying real and imaginary signals of the pure water class and σ_{w}^2 is the variance of the Gaussian noise in the individual signals, $I_0(\cdot)$ is the modified Bessel function of the first kind with order zero.

The parameters of the statistical model are estimated by using the method of maximum likelihood, the likelihood function to be maximized is the function $p(z)$ in Equation (6). Those parameters are the sub-model weights a_i ($i \in \{\mathrm{f}, \mathrm{m}, \mathrm{w}\}$), the weighting function $h(\alpha)$, the Rician parameters v_{w} and σ_{w}^2, the means and variances of the pure fat class in $\mathcal{I}_{\mathrm{f}}$ and $\mathcal{I}_{\mathrm{fw}}$, the mean and variance of the pure water class in $\mathcal{I}_{\mathrm{fw}}$, and the mean and variance of the pure water class in $\mathcal{I}_{\mathrm{f}}$. Once the parameters are estimated, we employ the maximum *a posteriori* (MAP) method to quantify the fat content in each voxel. As a final output of the algorithm, we aggregate these estimates into an α-image.

3. RESULTS

We construct a numerical phantom in a 3-D space that contains a portion of an ellipsoid. It is to mimic a part of a fat depot that is surrounded by water-predominated tissues in a biological object. A "fat only" image volume ($\mathcal{I}_{\mathrm{f}}$) and a "fat+water" image volume ($\mathcal{I}_{\mathrm{fw}}$) are synthesized at high resolution. If we treat the whole image volume as 1 unit, there is 0.4643 unit of fat in the phantom. Images are then downsampled into low resolution to help introduce partial volume averaging and mixture classes of different combinations of pure fat and pure water. Fig. 1(a) and Fig. 1(b) show the low resolution image of the numerical phantom and a synthetic ratio image $\mathcal{I}_{\mathrm{f}}/\mathcal{I}_{\mathrm{fw}}$, respectively. Synthetic data are generated with reference to real MRI data sets that contain images of a plastic bottle filled with half soybean oil and half deionized water.

A Monte Carlo hypothesis testing method is employed to test the validity of the statistical model and assess the goodness-of-fit. The Monte Carlo hypothesis testing begins with generating multiple realizations from the statistical model. Pearson's chi-square statistic is then computed for each realization. The distribution of the test statistic (denoted S) helps perform the null hypothesis H_0 testing: *the observed data is a realization of the model*. The P-value of the test is defined as,

$$\mathcal{P} = \Pr\left(S > s_{\mathrm{obs}} | H_0\right) \tag{9}$$

where s_{obs} is the test statistic value for the observed data. In addition to evaluating the model, we test the validity of the assumptions of the model. The assumptions are (1) coefficient of variation of the denominator distribution ($c.v.$) is small enough to justify the Gaussian approximation of the magnitude ratio distribution and (2) correlation coefficient of the numerator and denominator (ρ) can be neglected in the modeling. The null hypothesis is tested against different $c.v.$ and ρ values. Results are presented in Fig. 2. It is evident that the statistical model is valid over a wide range of $c.v.$ $(0 - 0.2)$ and ρ $(0 - 0.95)$, which cover the typical values in the MRI rat data sets that we have tested — $c.v.$: 0.063 for water and 0.027 for fat; ρ: 0.75 for water and 0.5 for fat.

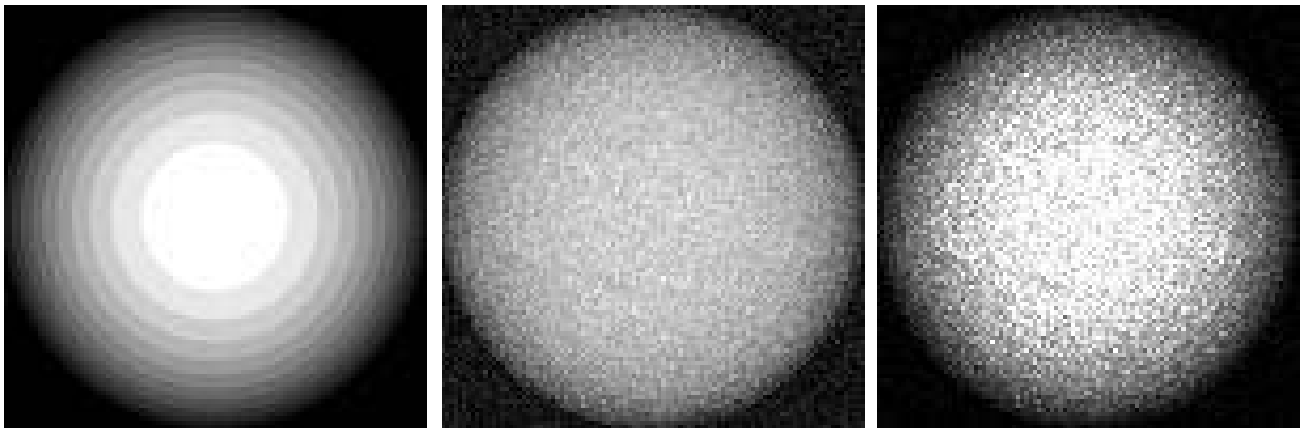

(a) Truth image (b) Ratio image (c) α-image

Fig. 1. (a) The low resolution image of the numerical phantom. (b) A synthetic ratio image $\mathcal{I}_{\text{f}}/\mathcal{I}_{\text{fw}}$, synthetic data are generated with reference to real MRI data sets that contain images of a plastic bottle filled with half soybean oil and half deionized water. (c) The maximum *a posteriori* (MAP) estimate, α-image.

Furthermore, we invalidate the linearity assumption on the relationship between the magnitude ratio and the percentage of fat visually by scatter plots and histograms. Numerical quantification with the Pearson's linear correlation coefficient (r) on the two quantities is also conducted. Fig. 3(a) (Fig. 3(b)) shows the plots and histograms between the magnitude ratio (α estimate) and the percentage of fat for the phantom data. It is illustrated that ratio intensity is not linearly related to the fat content ($r = 0.9527$), on the contrary, our α estimate is ($r = 0.9731$). This can be realized from the scattering of the points, the scatter points of ratio intensity are laid on arcs, whereas, the points of our α estimate are laid on straight lines that pass through the origin. For the MRI rat data sets (we have tested 6 data sets with genetically obese spontaneously hypertensive Koletsky rats), since the truth data is missing, we use the "fat only" image to approximate the truth. In order to reduce the effect from the receive coil sensitivity inhomogeneity, a small region of interest is used in the study. Similar results are observed, $r = 0.9632 \pm 0.0212$ for ratio intensity and $r = 0.9891 \pm 0.0097$ for α estimate. Fig. 1(c) shows the α-image of the phantom. The ratio and α-image of a MRI rat data set are given in Fig. 4.

Finally, we study the quantification of fat depots volume based upon the ratio images and the α-images with a simple thresholding method. The threshold used to segment the fat volume in a ratio image is the mid-point of the two peaks identified manually from the histogram, and we use 0.5 as the threshold to partition all the α-images. Thresholding the ratio image with the mid-value of the peaks assumes that there is a linearity with the fat content, whereas, thresholding with $\alpha = 0.5$ means that we classify a voxel as fat if there is more than 50% of its volume is fat. In case of rat data sets where no truth data are available, we use the total fat volume estimated from the "fat only" image as a reference, despite the fact that it is prone to under-estimation due to the receive coil sensitivity inhomogeneity. The mid-point of the two peaks in the histogram is used as a threshold to segment the fat volume. Results show that using ratio images for fat quantification tends to over-estimate the fat depot volume significantly, as compare to α-images, in the digital phantom (truth: 0.4643 unit; ratio intensity: 0.6619 unit [42.56% over-estimated]; α estimate: 0.4719 unit [1.64% over-estimated]). For the 6 MRI rat data sets, the reference total fat volume is $246 \pm 42\text{mL}$, thresholding the ratio images give $350 \pm 51\text{mL}$ ($\times 1.43 \pm 0.06$ of the reference volume) while the α estimate gives $279 \pm 45\text{mL}$ ($\times 1.13 \pm 0.02$ of the

reference volume). We concluded that our algorithm is capable of increasing the accuracy of the fat quantification using the MRI ratio imaging technique.

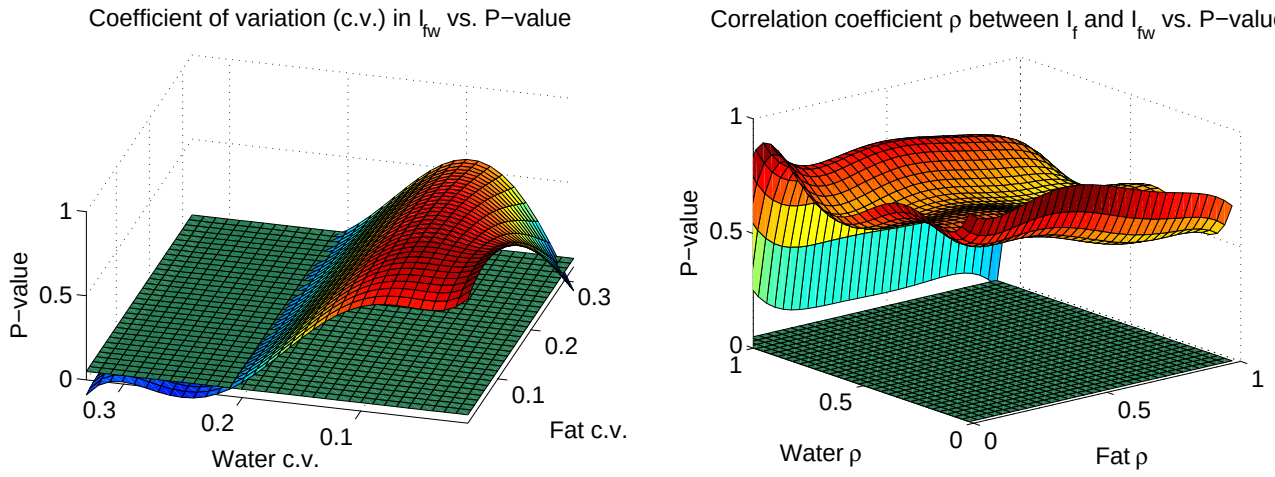

(a) Coeff. of variation $c.v.$ (b) Correlation coeff. ρ

Fig. 2. (a) Coefficient of variation of the denominator distribution ($c.v.$) vs. P-value. (b) Correlation coefficient of the numerator and denominator (ρ) vs. P-value. The flat surfaces are at P-value $= 0.05$, they show the significant level of the testing. It is evident that the statistical model is valid over a wide range of $c.v.$ $(0 - 0.2)$ and ρ $(0 - 0.95)$, which cover the typical values in the MRI rat data sets that we have tested — $c.v.$: 0.063 for water and 0.027 for fat; ρ: 0.75 for water and 0.5 for fat.

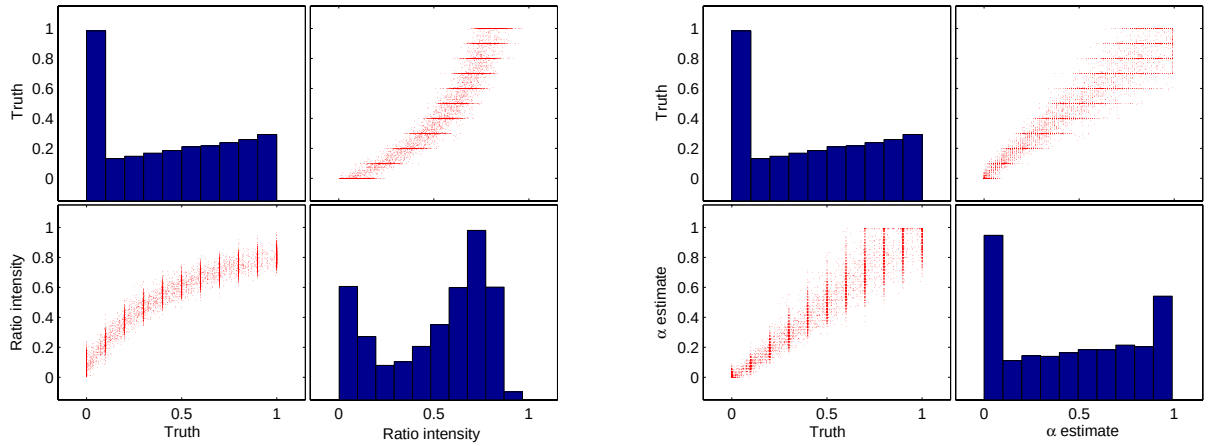

(a) Ratio intensity (b) α estimate

Fig. 3. (a) Scatter plots and histograms on the relationship between the ratio intensity and the percentage of fat for the phantom data. (b) Similar plots and histograms for our α estimate. It is illustrated that ratio intensity is not linearly related to the fat content (note that scatter points are laid on arcs, $r = 0.9527$), on the contrary, our α estimate is (points are laid on straight lines that pass through the origin, $r = 0.9731$). The linearity between the α estimate and the truth fat content can also be realized from their histograms, both histograms are very similar as shown in (b).

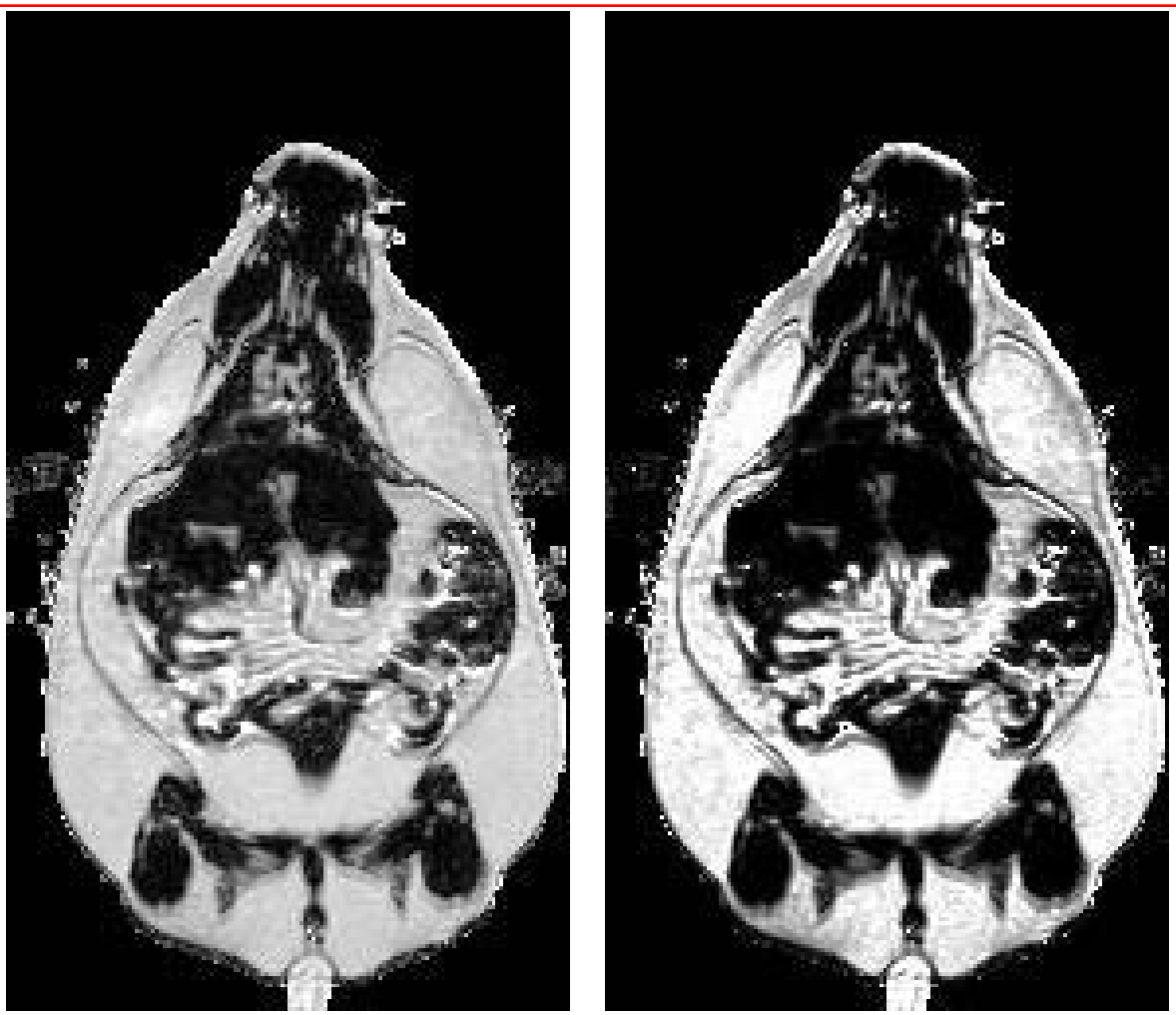

(a) Ratio intensity (b) α estimate

Fig. 4. The (a) ratio and (b) α-image of a MRI rat data set are presented. Both images are shown in the same brightness and contrast. It is evident that α estimate gives an image with a better contrast, whereas, signals are flat in the ratio image. As such, our α-image is capable of giving a clearer delineation of the water-fat boundary in addition to a more accurate volumetric quantification.

4. NEW OR BREAKTHROUGH WORK

We are the first group reporting the statistical model of the ratio images. The goodness-of-fit of the model is assessed with Monte Carlo hypothesis testing. We also invalidate the linearity assumption between the ratio intensity and the fat content per voxel. An algorithm, based upon a Bayesian formulation, to estimate the percentage of fat per voxel from the ratio images is finally proposed.

5. CONCLUSION

We have demonstrated a novel method to estimate the percentage of fat per voxel from the ratio images. Our estimate is capable of correcting the non-linearity relationship between the ratio intensity and the fat content and producing more accurate fat volume quantification than the ratio images with a simple thresholding method. Future work will include incorporation of non-uniform prior, such as a Markov random fields (MRF) smoothness prior, to provide better fat content estimation and increase robustness to noise.

ACKNOWLEDGMENT

This work was supported by the Ohio Wright Center/BRTT (The Biomedical Structure, Functional and Molecular Imaging Enterprise), NIH 5R01EB004070-03 (Quantitative Image Quality for Optimization of MRI) and NIH 1T32EB007509-01 (Interdisciplinary Biomedical Imaging Training Program).

REFERENCES

[1] D. S. Gray, K. Fujioka, P. M. Colletti, H. Kim, W. Devine, T. Cuyegkeng, and T. Pappas, "Magnetic-resonance imaging used for determining fat distribution in obesity and diabetes," *Am. J. Clin. Nutr.* **54**(4), pp. 623–627, 1991.
[2] E. Thomas, N. Saeed, J. Hajnal, A. Brynes, A. Goldstone, G. Frost, and J. Bell, "Magnetic resonance imaging of total body fat," *J. Appl. Physiol.* **85**, pp. 1778–1785, Nov. 1998.
[3] B. Wajchenberg, "Subcutaneous and visceral adipose tissue: their relation to the metabolic syndrome," *Endocrine Reviews* **21**(6), pp. 697–738, 2000.
[4] D. H. Johnson, C. Flask, D. Wan, P. Ernsberger, and D. L. Wilson, "Quantification of adipose tissue in a rodent model of obesity," in *SPIE Med. Imag.*, A. Manduca and A. A. Amini, eds., **6143**(1), pp. 2–11, SPIE, 2006.
[5] A. Haase, J. Frahm, W. Hanicke, and D. Matthaei, "^1H NMR chemical shift selective (CHESS) imaging," *Phys. Med. Biol.* **30**, pp. 341–344, Apr. 1985.
[6] H. Gudbjartsson and S. Patz, "The rician distribution of noisy MRI data," *Magnet. Reson. Med.* **34**, pp. 910–914, 1995.
[7] A. C. S. Chung and J. A. Noble, "Statistical 3D vessel segmentation using a rician distribution," in *Med. Imag. Comput. Comput. Assist. Interv., Lecture Notes in Comput. Sci.* **1679**, pp. 82–89, Berlin, Springer-Verlag, 1999.
[8] R. C. Geary, "The frequency distribution of the quotient of two normal variates," *J. Roy. Stat. Soc.* **93**(3), pp. 442–446, 1930.
[9] E. C. Fieller, "The distribution of the index in a normal bivariate population," *Biometrika* **24**(3/4), pp. 428–440, 1932.
[10] G. Marsaglia, "Ratios of normal variables and ratios of sums of uniform variables," *J. Am. Stat. Assoc.* **60**(309), pp. 193–204, 1965.
[11] D. V. Hinkley, "On the ratio of two correlated normal random variables," *Biometrika* **56**, pp. 635–639, Dec. 1969.
[12] J. Hayya, D. Armstrong, and N. Gressis, "A note on the ratio of two normally distributed variables," *Management Sci.* **21**, pp. 1338–1341, July 1975.
[13] P. Santago and H. Gage, "Quantification of mr brain images by mixture density and partial volume modeling," *IEEE Trans. Med. Imag.* **12**(3), pp. 566–574, 1993.